J Soils Sediments (2017) 17:1140–1159
DOI 10.1007/s11368-016-1601-4

SEDIMENTS, SEC 1 • SEDIMENT QUALITY AND IMPACT ASSESSMENT • RESEARCH ARTICLE

A numerical framework for modelling sediment and chemical constituents transport in the Lower Athabasca River

Ahmad Shakibaeinia[1,2] · **Yonas B. Dibike**[2] · **Shalini Kashyap**[2,3] · **Terry D. Prowse**[2] · **Ian G. Droppo**[4]

Received: 22 February 2016 / Accepted: 6 November 2016 / Published online: 21 November 2016

Abstract
Purpose The transport of fine sediments and associated chemical constituents originating from potential anthropogenic and natural sources is becoming an issue of increasing importance in the Lower Athabasca River (LAR) ecosystem in northern Alberta, Canada. This study aims to (1) establish an integrated numerical modelling framework to investigate the transport of fine cohesive sediments and associated chemical constituents during both ice-covered and open-water periods and (2) apply the modelling framework to investigate the state and temporal/spatial variation in sediment and selected chemical constituents within the LAR.
Materials and methods One-dimensional hydrodynamic and transport models, combined with a river ice model, are used to predict the flow characteristics, transport of sediments and a selection of three metals and three polycyclic aromatic hydrocarbons (PAHs) within a ~200 km reach of the LAR, both in open-water and ice-covered conditions. The models are validated using available field measurements and are applied to investigate the state and variation of sediment and chemicals for a baseline period as well as to assess the effect of various hypothetical pollution scenarios.
Results and discussion The model simulations successfully reproduce the hydrodynamics and sediment transport patterns as well as the state and variation of selected metal and PAH constituents. The results generally show that the concentration of chemical constituents in the bed sediment is the major factor in determining the state and variation of their concentration in the water column, and the high-flow season is the critical period for the transport of sediment and chemicals in the system. The scenario simulation results indicate that increases in the concentrations of chemical constituents in tributary streams have to be orders of magnitude higher to have a noticeable effect on their corresponding water column concentration in the LAR. Those effects are also found to be higher only within the immediate vicinity of the tributary confluences and gradually diminish with distance downstream of the confluences.
Conclusions The numerical modelling framework developed in this study provides a tool for investigation and understanding of the state and temporal/spatial variation of sediment and associated chemical constituents within cold region rivers such as the LAR. By conducting additional scenario-based studies (such as future climate and chemicals loading), the models can be used to identify possible future states of sediment and water quality constituents in the LAR ecosystem.

Keywords Chemical transport · Cold season effect · Lower Athabasca River · Numerical modelling · Sediment transport

Responsible editor: Kimberley N. Irvine

Electronic supplementary material The online version of this article (doi:10.1007/s11368-016-1601-4) contains supplementary material, which is available to authorized users.

✉ Ahmad Shakibaeinia
ahmad.shakibaeinia@polymtl.ca

[1] Department of Civil, Geological and Mining Eng, Polytechnique Montreal, Montreal, Canada

[2] Environment and Climate Change Canada, Water & Climate Impact Research Centre (W-CIRC), Victoria, Canada

[3] Environment and Climate Change Canada, Canadian Centre for Inland Waters (CCIW), Burlington, Canada

[4] Alberta Environment and Parks, Edmonton, Canada

1 Introduction

The Lower Athabasca River (LAR), in northern Alberta, Canada, begins north of Fort McMurray and flows to the

Athabasca Delta and Lake Athabasca. Throughout its course, the river cuts through natural bitumen deposits (Conly et al. 2002) and runs adjacent to the oil sands developments. Fine cohesive sediments and associated chemical constituents such as metals and polycyclic aromatic hydrocarbons (PAHs) play an important role in the LAR ecosystem (Ghosh et al. 2000; Garcia-Aragon et al. 2011). Therefore, there is a great demand to characterize the contribution of bitumen deposits to the sediments and chemicals in Athabasca River system. Experimental assessment of cohesive sediment deposition dynamics in Athabasca River and tributaries has been the subject of a number of recent studies (e.g. Garcia-Aragon et al. 2011; Droppo et al. 2014; Droppo and Krishnappan 2014). A sediment budget analysis (using available field data) by Conly et al. (2002) found that suspended sediment derived from tributary sources and the bed erosion within the LAR each account for about 10% of the mean annual load of the Athabasca River with the remaining 80% coming from upstream of this lower reach.

Wrona et al. (2000) described the contaminant sources, distribution and fate in the Northern Rivers, including Athabasca River, concluding that the levels of most of the contaminants are mostly within the Canadian or provincial guidelines for both aquatic and human health. Headley et al. (2001) analyzed the characteristics of the natural source of hydrocarbons originating in the tributaries to the LAR and found that tributaries, particularly Steepbank River, Ells River and MacKay River, contain significant levels of naturally derived PAHs; however, the levels fall rapidly when tributaries converge with the main stem. Akre et al. (2004) also investigated the spatial patterns of natural PAH sediment in the LAR. Conly et al. (2007) showed that there is no significant trend of metal concentration in tributaries from upstream to the downstream of the development. However, some studies have shown that PAH and metal concentration in the LAR are affected by the oil sands development activities (e.g. Timoney and Lee 2009; Kelly et al. 2010; Wiklund et al. 2014). Timoney and Lee (2009) investigated the potential of pollution from oil sands industrial activities and concluded that the levels of most PAH and metal constituents have increased downstream of oil sands developments. Kelly et al. (2010) also showed that during summer, the concentration of 13 metal constituents (considered as priority pollutants under the US Environmental Protection Agency (EPA)) near the oil sands developments is greater than that of upstream of developments. Wiklund et al. (2014), by analyzing metal concentrations in sediments deposited in floodplain lakes of the Athabasca Delta during 1700–1916, characterized preindustrial reference metal concentrations in sediment downstream of Alberta oil sands. Hall et al. (2012) found that the natural erosion of exposed bitumen in banks of the Athabasca River (of main stem and its tributaries) is a major source of polycyclic aromatic compounds (PACs) to the Athabasca Delta. There have also been many documented incidences of industrial pollutions or degradation, including several spills into the LAR as well as Muskeg and Ells Rivers (Timoney and Lee 2009).

Numerical models can be effective tools to predict the erosion, transport and fate of sediments and associated chemical constituents within various river environments. However, modelling of flow and sediments in the LAR is challenging due to its complex morphology and highly seasonal flow reflecting the hydroclimatic condition in the region. Being located in a cold region environment, ice formation, breakup and the relatively long ice cover period can further complicate the modelling, as ice processes can significantly change flow and geomorphic processes (Prowse 2001; Ettema and Daly 2004). Khanna and Herrera (2003), Andrishak et al. (2008) and Pietroniro et al. (2011) made early attempts to model flow in LAR using a one-dimensional (1D) model, which incorporated simplified rectangular sections to represent channel geometry. More recently, Shakibaeinia et al. (2016) and Kashyap et al. (2014) made the first effort to develop an integrated numerical modelling framework (1D and 2D) for simulation of flow, ice processes and water quality in LAR using the detailed surveyed bathymetry.

Despite the great deal of research, the current state and spatial and temporal evolution of the sediments and associated chemical constituents as well as the effects on the transport mechanisms of cold season river ice cover in LAR are not yet well understood. The focus of most of the previous studies has been based on limited measured data and mostly during the open-water season. Therefore, the Canada-Alberta Joint Oil-Sands Monitoring Program (2012) identified a need for a more systematic and comprehensive quantification and modelling of the sources, transport, flux and fate of materials and chemical constituents entering the Lower Athabasca watersheds. To achieve this objective, it was required to develop a reliable integrated hydrodynamic, sediment transport and water quality models of the LAR.

This study aims to develop such an integrated 1D deterministic numerical modelling framework to investigate the spatial and temporal variation in the sediment regime and associated PAH and metal constituents in LAR for both open-water and ice-covered conditions. The proposed numerical framework for the study is summarized in Fig. 1. A 1D model (Mike-11) is used for large-scale long-term simulation of flow hydrodynamics and sediment transport patterns in the LAR. Furthermore, a 1D ice model (CRISSP 1D) is used to predict the winter ice coverage and its effect on the river flow characteristics; however, other ice processes (such as ice breakup) are not taken into account. The results of the ice model are used to modify the sediment transport and hydrodynamic

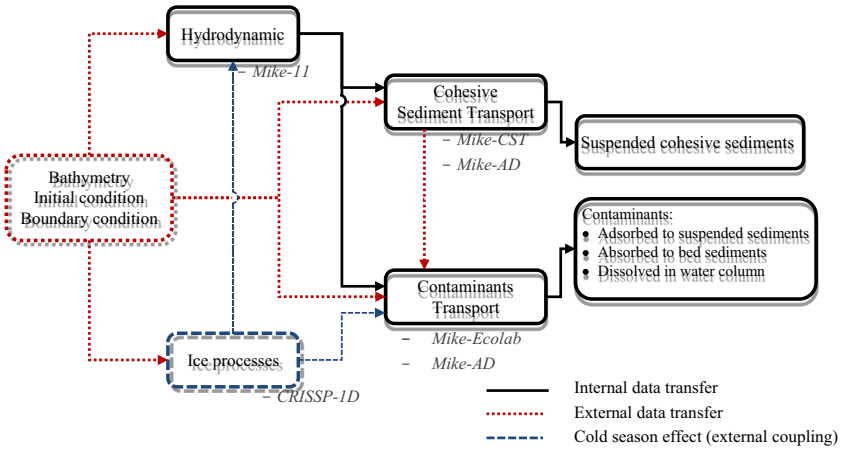

Fig. 1 Numerical modelling framework of the present study

models to account for the effect of winter ice cover. The sediment transport simulations serve as the basis for setting up contaminant transport models for a selection of three PAH (pyrene (PY), phenantrene (Ph) and C1-benz[a]anthracenes/chrysenes (BAC1)) and three metal (lead (Pb), arsenic (As) and vanadium (V)) constituents. The validated models are also applied to investigate the effect of some hypothetical pollution scenarios on the water column concentration of two selected chemicals, PY and lead (Pb) within the LAR.

2 Numerical models

2.1 Hydrodynamics

The 1D numerical modelling system used for this study is the Mike-11 (Danish Hydraulics Institute, DHI 2012). Mike-11 hydrodynamic module (HD) solves the shallow flow equations (Saint Venant's equations), using an implicit finite difference method and the six-point Abbott scheme (DHI 2012). The 1D (area averaged) equations for conservation of mass and momentum are given by

$$\begin{cases} \dfrac{\partial A}{\partial t}+\dfrac{\partial Q}{\partial x}=q \\ \dfrac{\partial Q}{\partial t}+\dfrac{\partial}{\partial x}\left(\dfrac{\alpha Q^2}{A}\right)+gA\dfrac{\partial h}{\partial x}+\dfrac{gn^2Q|Q|}{AR^{4/3}}=0 \end{cases} \quad (1)$$

where Q is the discharge, A is the flow area, q is the lateral inflow, h is the stage above datum, R is the hydraulic radius, α is the momentum distribution coefficient, and n is Manning's coefficient. The hydraulic radius formulation is based on a parallel channel analysis where the total conveyance of the section at a given elevation is equal to the sum of the conveyances of the parallel channels.

2.2 Fine-sediment transport model

The advection-dispersion (AD) and cohesive sediment transport (CST) modelling modules of Mike-11 are used for the purpose of fine-sediment transport modelling. The AD module is based on the 1D equation of conservation of mass (of dissolved or suspended materials). This module uses the outputs of the HD (e.g. discharge and water level, cross-sectional area and hydraulic radius). The CST module is coupled with the AD module and is used to describe the transport of suspended fine sediments. The erosion/deposition is considered as a sink/source term of the AD equations. Conservation of mass of sediment particles and flocs, i.e. the AD equation, is given by

$$\frac{\partial c}{\partial t}+u_i\frac{\partial c}{\partial x_i}-\frac{\partial}{\partial x_i}\left(D\frac{\partial c}{\partial x_i}\right)=S \quad (2)$$

The area averaged 1D equation (used in Mike-11) is then derived as

$$\frac{\partial Ac}{\partial t}+\frac{\partial Qc}{\partial x}-\frac{\partial}{\partial x}\left(AD\frac{\partial c}{\partial x}\right)=AKc+c_2q \quad (3)$$

where c is the concentration, D is the dispersion coefficient, u_i is the velocity component in i direction, S represents the sink/source terms, A is the cross-sectional area, K is the linear decay coefficient, c_2 is the source/sink concentration, q is the lateral inflow, x is the space coordinate, and t is the time coordinate. Sediment deposition (S_d) and erosion (S_e) are the two main source/sink terms in AD equations. Deposition of suspended sediment particles and flocs occurs when the mean flow velocity is sufficiently low so that the corresponding bed shear stress, τ_b, is less than the critical shear stress for deposition, τ_{cd}, that would result in the particles and flocs to fall to the bed and remain there (without becoming resuspended immediately). On the other hand, the river bed will erode when the bed shear stress, τ_b, exceeds a critical shear stress for

erosion, τ_{ce}. The deposition and erosion rates S_d and S_e can be expressed by Van Rijn (1984):

$$S_d = W_s c\left(\frac{\tau_{cd}-\tau_b}{\tau_{cd}}\right) \text{ if } \tau_b \le \tau_{cd}, \text{ and } S_d = 0 \text{ if } \tau_b > \tau_{cd} \quad (4)$$

$$S_e = E_0\left(\frac{\tau_b-\tau_{ce}}{\tau_{ce}}\right)^n \text{ if } \tau_b \ge \tau_{ce}, \text{ and } S_e = 0 \text{ if } \tau_b < \tau_{ce} \quad (5)$$

where W_s is the settling velocity of sediments and E_0 and n are the erosion coefficient and exponent, respectively. The erosion rate and critical shear stress values used in this study are based on physical laboratory experiments conducted (in a circular flume) on sampled bed materials collected from the Lower Athabasca region (Droppo et al. 2014). However, the measured erosion rates are limited to lower values of bed shear stress; therefore, they are extended to cover higher shear stress values using a third-order polynomial function (see Electronic Supplementary Material, Fig. S1). The local bed shear stress can be given by

$$\tau_b = \rho g(V/C_{ch})^2 = \rho g(nV)^2/h^{1/3} \quad (6)$$

where C_{ch} is the Chezy resistance number, h is the flow depth, n is Manning's number, and V is the flow velocity. Settling velocity of flocs is an important parameter in the description of the cohesive sediment transport. In Mike-11, two settling regimes are considered. The first regime considers the effect of flocculation on settling velocity. Below a user-specified concentration, C_{v0}, the settling velocity usually increases with concentration due to the increase in the floc size. However, an increase in sediment concentration above the specified level causes a decrease in settling velocity due to the hindered settling effect. The settling velocity is expressed by

$$\begin{cases} W_s = kC_v^m & C_v \le C_{v0} \\ W_s = W_0(1-C_v)^\gamma & C_v \ge C_{v0} \end{cases} \quad (7)$$

where C_v is the volume concentration, W_0 is the free settling velocity, m and γ are the exponent factors, and k is a coefficient that can be calculated by $k = W_0(1-C_{v0})^\gamma/C_{v0}^m$. In this 1D model, the vertical velocity distribution is assumed to be uniform (an ideal mixing). Mike-11 can include up to three sediment layers at the bed. Both hindered settling and consolidation are considered in the process of transition from layers 1 to 2 and from layers 2 to 3. Note that flocculation process is not explicitly accounted in the numerical models used for this study. Nevertheless, experimental and numerical results of Droppo and Krishnappan (2014) have shown that, considering the flow and sediment characteristics, flocculation processes are not likely to influence sediment transport characteristics in the LAR and tributaries. The sediment/floc size is implicitly considered in the model by its effect on parameters such as settling velocity, critical shear stress and erosion rate.

2.3 Chemical constituents

The Mike-11 chemical constituents' model couples some built-in numerical lab templates, called ECO Labs (which deal with transforming processes of components) with an AD module (which handles the simultaneous transport processes). Xenobiotics (XE) and heavy-metal (HM) templates are two of Mike-11 ECO Lab templates that are used in this study for simulation of PAH and metal constituents, respectively. Both templates share the same description of adsorption, desorption, advection and diffusion. The HM template accounts for the adsorption and desorption of chemicals, sedimentation and resuspension of particulate chemicals, diffusive transport of dissolved chemical at the sediment/water interface and transport of dissolved and particulate chemicals in the water column by advection and dispersion. The XE template is similar to the HM template, except that it also accounts for chemical degradation processes such as biodegradation, photolysis, hydrolysis and evaporation of dissolved chemicals, which make it more appropriate for the simulation of the PAHs (DHI 2012).

The sediment properties (e.g. porosity and density) are assumed to remain constant, and the sedimentation/resuspension process only changes the sediment layer thickness. The state variables considered here are as follows: dissolved concentration in water, D_w, adsorbed concentration in water, A_w, dissolved concentration in bed sediments, D_s, adsorbed concentration in bed sediments, A_s, and suspended sediment concentration, c. Note that the XE and HM templates have a simple built-in sediment transport model and cannot be internally coupled with the cohesive sediment transport (CST) modelling module. Therefore, here, we calibrate the results of sediment transport within XE and HM templates with those achieved from the CST module. The summary of the governing equations for distribution and transformation process within the Mike-11 XE and HM templates has been provided in Table 1.

The adsorption/desorption processes are described using a partitioning coefficient, K_d. K_d (l kg^{-1}) is defined as the ratio of a chemical's concentration (mg kg^{-1}) adsorbed to the particulate (sediment) phase to the concentration (mg l^{-1}) dissolved in the water phase at equilibrium. For the organic part of the sediments (PAHs are mostly bounded to the organic part of the sediments), the K_d is estimated from a normalized partitioning coefficient K_{oc} as

$$K_d = f_{oc} \cdot K_{oc} \quad (8)$$

Table 1 A summary of the state variables and differential equation within the XE and HM templates

State variable	Differential equation*
Dissolved chemical in water column	$\frac{\partial D_w}{\partial t} = -\overbrace{k_w K_{dw} D_w c}^{adsorption} + \overbrace{k_w A_w}^{desorption} + \overbrace{\varepsilon \frac{\left(D_s/\left(\eta\, dz_s\right) - D_w\right)}{\left(dz_f + dz_s\right) dz}}^{diffusion} - \overbrace{d_B + d_H + d_P}^{degredation} + \overbrace{k_{ev} D_w / dz}^{evaporation}$
Adsorbed chemical in water column	$\frac{\partial A_w}{\partial t} = \overbrace{k_w K_{dw} D_w c}^{adsorption} - \overbrace{k_w A_w}^{desorption} - \overbrace{W_s A_w / dz}^{sedimentation} + \overbrace{R_s / \left(M_s dz\right)}^{resuspension}$
Dissolved chemical in bed sediments	$\frac{\partial D_s}{\partial t} = -\overbrace{k_s K_{ds} D_s\, M_s / \left(n\, dz_s\right)}^{adsorption} + \overbrace{k_s A_s}^{desorption} + \overbrace{\varepsilon \frac{\left(D_w/\left(\eta\, dz_s\right) - D_w\right)}{dz_f + dz_s}}^{diffusion} - \overbrace{d_B + d_H}^{degredation}$
Adsorbed chemical in bed sediment	$\frac{\partial A_s}{\partial t} = \overbrace{k_s K_{ds} D_s\, M_s / \left(n\, dz_s\right)}^{adsorption} - \overbrace{k_s A_s}^{desorption} + \overbrace{W_s A_w / dz}^{sedimentation} - \overbrace{R_s A_s / \left(M_s dz\right)}^{resuspension}$
TSS	$\frac{\partial c}{\partial t} = \overbrace{W_s c / dz}^{sedimentation} - \overbrace{R_s / dz}^{resuspension\ (if\ U > u_c)} + \overbrace{R_p / dz}^{Production}$

[a] K_{dw} and K_{ds} are the partitioning coefficients in water column and bed sediments, respectively; k_s and k_w are the desorption rates in bed sediment and water column, respectively; R_s is the suspension rate of sediments (~ erosion rate used in Eq. 5); R_p is the particle production rate; M_s is the mass of sediments; η is the porosity; dz, dz_s and dz_f are the thicknesses of computational grid, sediment layer and water film, respectively; d_B, d_H and d_P account for bio-decay, hydrolysis and photolysis, respectively; ε is the diffusion coefficient, k_{ev} is the evaporation rate, W_s is the sediment settling velocity; and u_c is the critical velocity for resuspension (calculated from the critical shear stress)

where f_{oc} is the fraction organic carbon in sediments (mg mg^{-1}). K_{oc} is typically measured at the same pH and salinity of the study river and is different for each of the chemical constituents. Other partitioning coefficient relating the adsorption rate k_a (l kg^{-1} day^{-1}) and desorption rate in water column (suspended) sediments k_w (day^{-1}) and in bed sediment k_s (day^{-1}) as

$$K_{dw} = k_a/k_w \\ K_{ds} = k_a/k_s \quad (9)$$

K_{dw} and K_{ds} are partitioning coefficients in water column and bed sediments, respectively.

2.4 Cold season effects and river ice model

Ice processes (e.g. ice formation, coverage and breakup) can affect flow and sediment transport in cold region rivers (Prowse 2001; Knack and Shen 2015). Ice cover replaces the surficial wind shear stress with an under-ice shear stress, resulting in an increase in flow resistance and water level and a corresponding decrease in bulk velocity and bed shear stress (Ettema and Daly 2004). Such changes can reduce the rate of bed sediment transport. Mike-11 sediment transport models do not have internally coupled ice process models. Therefore, an external coupling approach is used in this study, where the simulated results from an ice process model (i.e. CRISSP1D, Shen 2005) are used to modify some relevant flow parameters in the hydrodynamic and sediment transport models, in order to account for the effect of ice coverage.

The CRISSP-1D model is used to predict the temporal and spatial variation of ice coverage within the study reach. The model simulates unsteady flows in single or complex channel networks using a four-point implicit finite difference method (Shen 2005). The model is able to simulate different ice processes including water temperature and concentration distributions of suspended and surface ice; ice cover formation, progression and consolidation; undercover transport and accumulation; ice jam; and ice break-up.

Change in flow resistance due to ice friction is taken into account (in Mike-11 models) by reproducing the under-ice shear stress τ_{ice}, as simulated by CRISSP-1D, and limiting the other surficial shear stresses τ_s (e.g. wind stress). The modified surface shear stress τ_s' is described as

$$\tau_s' = \psi \tau_{ice} + (1-\psi)\tau_s \quad (10)$$

$$\tau_{ice} = -\rho f_i |U| U/8 \quad (11)$$

where ψ $(x, t) \in [0, 1]$ is the ice surficial coverage, f_i is the ice friction coefficient, and U is the average flow velocity magnitude. For the contaminant transport, the temperature-related effect of cold season is automatically considered. The results of the ice process model are also used to modify any processes that involve mass exchange through water surface (e.g. aeration and evaporation).

3 Study area

3.1 Site description

The Athabasca River originates in the Rocky Mountains of Alberta, and it drains approximately 133,000-km^2 area above the city of Fort McMurray. The study reach is the lower portion of the Athabasca River (LAR) starting from below the confluence of Athabasca and Clearwater Rivers (near Fort McMurray) extending for ~200 km to Old Fort (Fig. 2). The river geometry is complex, as it contains vegetated islands, alternating sand bars and a bed, which is composed of a mixture of gravel, sand and cohesive sediment. This section of the river has been characterized as being somewhere between a meandering and a braided river and flows through natural oil sands formations where bitumen is found very close to the earth surface and is likely to be affected by natural erosional and depositional processes. This river reach also passes through the Lower Athabasca oil sands development area and the major tributaries contributing within the study reach are Steepbank, Ells, MacKay, Muskeg and Firebag Rivers.

3.2 River bathymetry data

River bathymetry data for the LAR were obtained from different sources, including (in order of priority in case of overlap) the following: (a) about ~40-km high-resolution (0.05 m) bathymetry data between Fort McMurray and Old Fort collected by Environment Canada (during 2012–2014 using a GeoSwath sonar sensor), (b) some detailed surveyed cross sections between Crooked Rapids and Steepbank River collected by Faye Hicks (2011), (c) six high-resolution surveyed

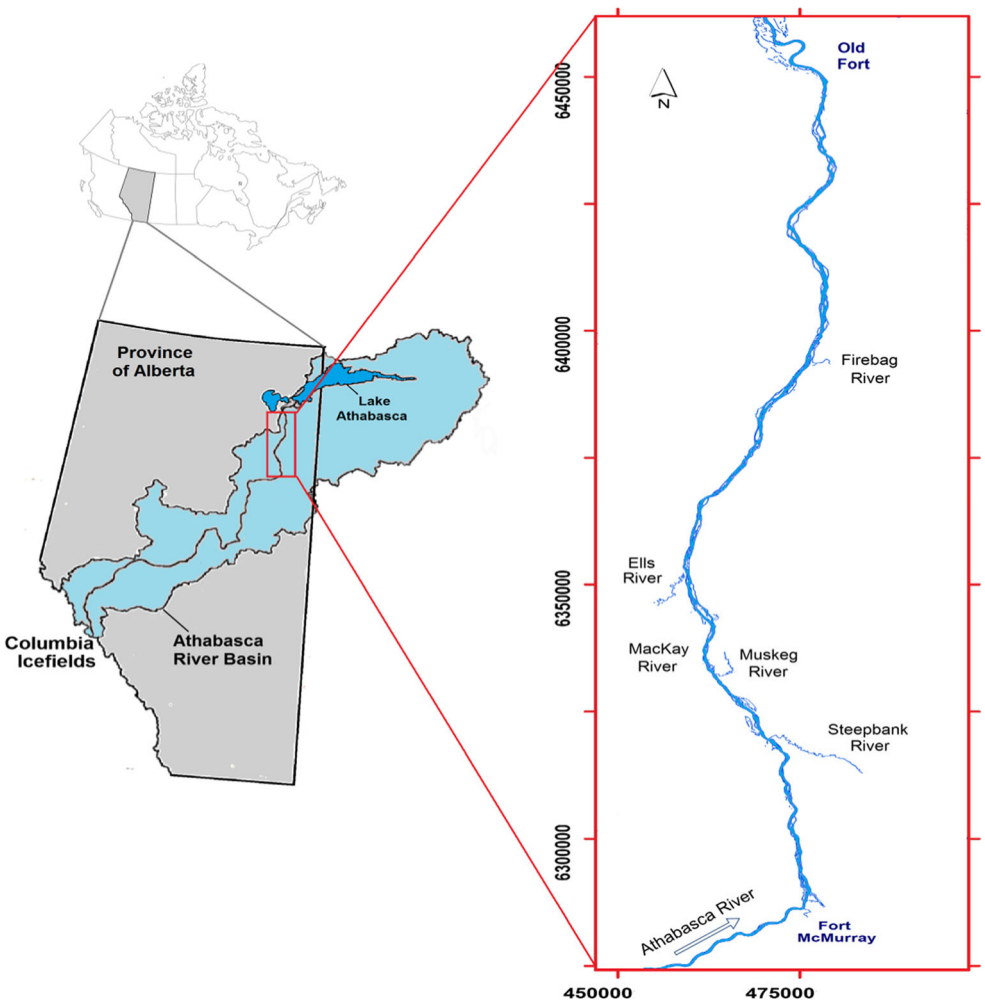

Fig. 2 Study river reach (Lower Athabasca River)

reaches collected by CEMA (2012) (using a Raytheon Fathometer echo sounder), (d) 127 digital elevation model (DEM) synthetic sections (~1-km intervals) between Steepbank River and Embarrass Airport obtained from the Mackenzie River Basin Hydraulic Model (Pietroniro et al. 2011), (e) high-resolution (5 m) light detection and ranging (LiDAR) data along the banks of the LAR provided by Alberta Environment and Sustainable Resources Development (AESRD), and (f) The DEM data of the region (Geobase 2012).

The bathymetry data from all these sources were combined to construct a continuous bathymetry for the LAR main channel and adjacent flood plains with a resolution ranging from 10 to 25 m. The LiDAR and DEM data were used to produce the topography of the river banks, flood plain and islands (area where other bathymetry sources have no coverage). Figure 3 shows the combined bathymetry elevation for the study reach and its flood plain. These bathymetry data were interpolated on the 1D cross sections (200 cross sections with ~1-km intervals) to construct the required model geometry.

3.3 Hydrometric and climate data

The hydrometric data (flow rates and water levels) used as model boundary conditions as well as for the purpose of model calibration and validation were obtained mainly from three different sources. Daily river flow and water-level data along the main stream and at major tributaries (near the confluence) were derived from Water Survey Canada (WSC 2013) hydrometric stations. The stations include (not limited to) the Athabasca River stations 07DD011 (near Old Fort), 07DA001 (below Fort McMurray), 07DA003 (near Fort Mackay) and 07DD001 (at the Embarras Airport) (Fig. 3). Additional flow and water-level data along the river, including stations S24 (below Eymundson Creek) and S46 (bellow Embarras airport), were obtained from Regional Aquatics Monitoring Program (RAMP 2013) hydrology stations. Simulated flow data from the Variable Infiltration Capacity (VIC) hydrologic model of the Athabasca watershed developed by Environment Canada (Eum et al. 2014) were also used for smaller tributaries where there are no hydrometric stations for flow measurements. Climate data required for

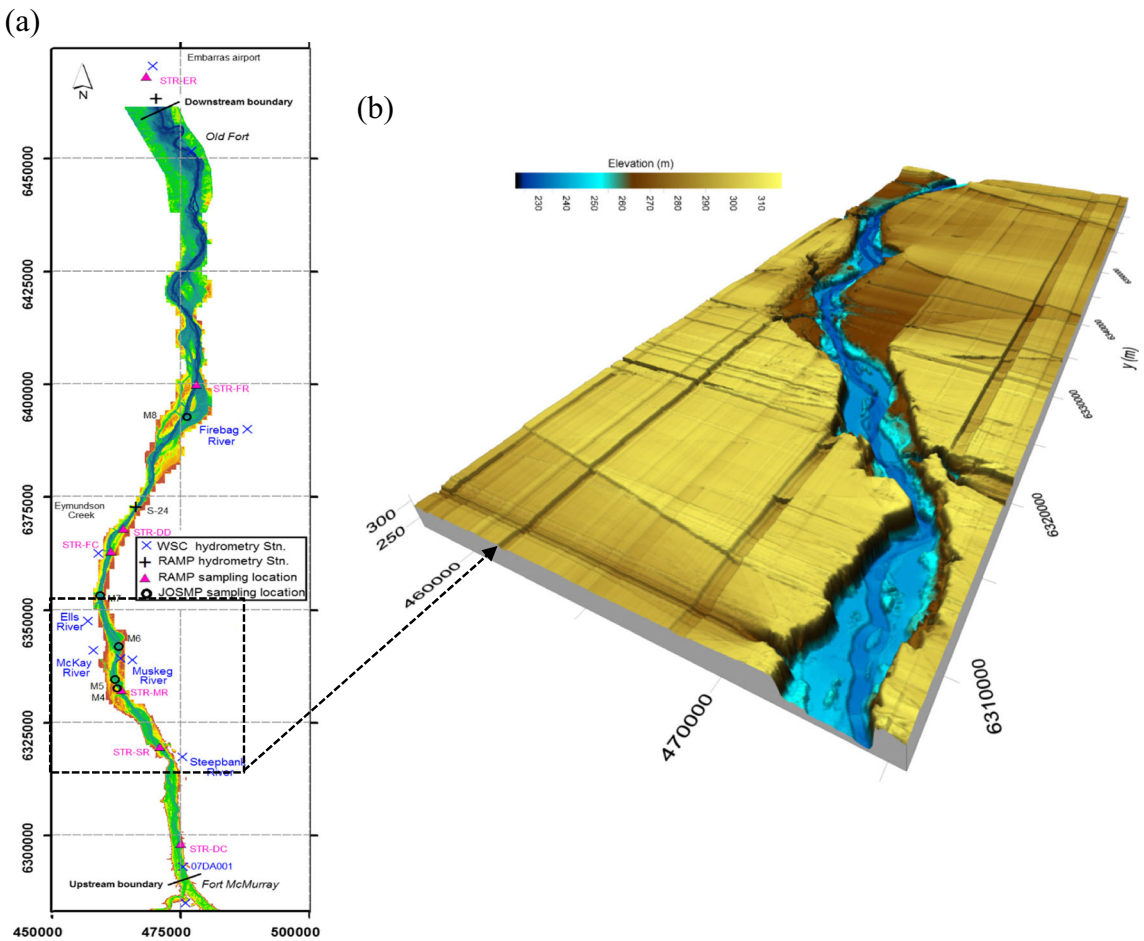

Fig. 3 Combined bathymetry of the LAR (for the main stem and adjoining flood plain) including the locations of the hydrometric and water quality measurement stations: **a** 2D plot of whole study reach and **b** 3D view of a selected reach

the study, such as air temperature (daily and hourly), wind speed, cloud coverage and precipitation, were obtained from Environment Canada climate database (EC 2013) for stations along the Lower Athabasca main stream.

Examples of available hydrometric data for the study reach are provided in the Electronic Supplementary Material (Fig. S2). The daily mean flow rate of the Athabasca River below Fort McMurray (the upstream boundary of the study reach) during the 2000–2012 simulation period is 510 $m^3 s^{-1}$. During the same period, the mean daily temperature in the cold season reached to −25 °C and the cold season (below zero) extends from around October to April.

3.4 Sediment and chemical constituent data

Suspended sediment concentrations used for boundary/initial conditions as well as for validation purposes are taken from Water Survey of Canada (WSC 2013) hydrometric stations along the main stream and at major tributaries (near the confluence). Besides, RAMP (2013) sediment data were also used when and where available. The required data for chemical constituents in the bed sediment and water column are also taken from RAMP (2013). Furthermore, since 2011, the Joint Oil-Sands Monitoring Program (JOSMP), a collaborative effort by Environment Canada and the province of Alberta (JOSMP 2015), has been collecting continuous water quality data for numerous sampling locations (including M4 to M8 as shown in Fig. 4) along the LAR and its tributaries. Figure 3 shows the location of some of the data collation sites.

Table 2 summarizes the average measured mass inflow (concentration multiplied by discharge) of example chemical constituents in the water column for the main stem (at upstream boundary of the study reach) and at the confluences of major tributaries. While the data generally belong to the 1997 to 2012 period, however, most of the PAH data were collected during the open-water seasons of 2011 and 2012. Because of the relatively large differences in the flow discharge, the mass inflow from the tributaries is small compared to those of the main stem.

The measurements for suspended sediment and constituent chemical concentrations (in water column) in the Athabasca River main channel and its tributaries are usually taken at various frequencies covering different time periods. Hence, continuous time series data that can be used directly as upstream and lateral boundary conditions are not available. Instead, the available observed data are used to develop rating curves relating sediment and constituent chemical concentrations with the corresponding flow rates that can then be used to generate continuous time series data for the inflow boundary conditions as well as for validation of the model results. Figure 4 shows the examples of such rating curves developed for the upstream boundary (below Fort McMurray) and at the confluence of one of the major tributaries (for both ice-covered and open-water conditions). Similarly, Fig. 5 shows the example rating curves developed for two of the chemical constituents (lead and PY) at the Athabasca River upstream boundary. In general, these figures show a relatively good correlation (see R^2 factor) between discharge and sediment/chemical constituent concentration values. The longitudinal variations in the average measured concentrations in bed sediments for the six chemical constituents are also presented in Fig. 6 showing relatively higher bed concentrations at upstream half (near the oil sands developments) of the study reach.

4 Model settings

The combined bathymetry of the ~200-km study reach between Fort McMurray and Old Fort (see Sect. 3.2) was evenly divided into 200 interpolated cross sections (with average width of 4- at 1-km interval). Abrupt changes in the longitudinal bed profile were smoothed to improve the stability of the implemented ice model. A simulation period from 2000 to 2011 was selected based on the availability of data for model boundary conditions as well as model calibration/validation. A spatially variable Manning coefficient (calibrated based on the bed materials) is used. The flow boundary conditions

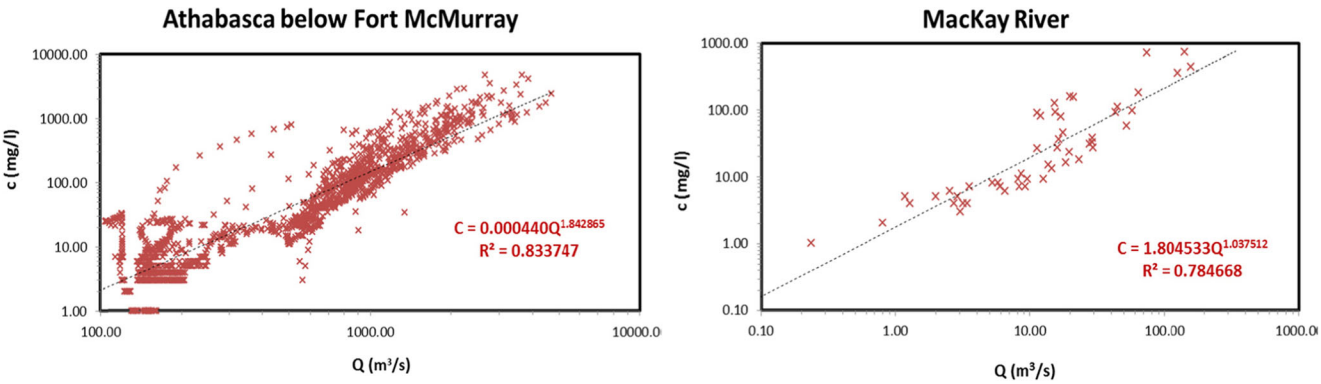

Fig. 4 Examples of suspended sediment rating curves for the Athabasca River below Fort McMurray and for the MacKay River at the confluence

Table 2 Average mass inflow of selected chemical constituents, including pyrene (PY), phenantrene (Ph), C1-benz[a]anthracenes/chrysenes (BAC1), lead (Pb), arsenic (As) and vanadium (V) in the Lower Athabasca main stem and major tributaries

	Mass inflow (g day^{-1})					
	PY	Ph	BAC1	V	Pb	As
Athabasca (U/S boundary)	174.1	272.3	613.1	186,264	56,024	53,512
Steepbank River	5.4	3.8	29.5	802	386	405
Muskeg River	0.3	0.5	0.6	292	96	257
MacKay River	3.0	2.6	13.7	2894	629	1500
Ells River	1.7	1.0	3.6	1303	297	609
Firebag River	3.4	2.8	7.7	1717	488	1182

Generally, the values are based on the available data in the period of 1997 to 2012

include time series of flow rates at the inflow boundaries (mainstem upstream boundary and confluences of tributaries) and water level at the outflow boundary (near Old Fort). Boundary conditions for the ice models include the time series of water temperature, ice concentration, ice thickness at the inflows and open transport ($dc/dx = 0$) condition at the outflow. The other input data include air temperature, wind speed and cloudiness percent along the reach. For the fine-sediment transport model, the time series of sediment concentration was used at the inflow boundaries and open transport for the outflow.

For the contaminant transport model, the derived time series (see Sect. 3.4) for suspended sediments as well as adsorbed and dissolved concentrations of each chemical constituent in the water column were employed at the inflow boundaries. The initial states of concentration in the water column and bed sediments were also assigned based on the averaged measured data for year 2000. The three metal constituents, namely, lead (Pb), arsenic (As) and vanadium (V), and the three PAH constituents (two parent and one alkylated), pyrene (PY), phenantrene (Ph) and C1-benz[a]anthracenes/chrysenes (BAC1), are selected for simulation purpose based on the data availability (for boundary/initial condition and validation), their increasing trend (from upstream to downstream of oil sands developments) and also recommendation on their relative importance from literature (e.g. Timoney and Lee 2009). The contaminant transport model parameters were calibrated within the expected values/ranges found in the literature. Summary of parameters, their expected ranges and calibrated values are presented in the Electronic Supplementary Material (Table S1).

5 Results and discussion

5.1 1D hydrodynamics and river ice modelling

To evaluate the performance of the flow and river ice models, the simulated water levels in open-water and ice-covered conditions are compared to that of the available measurements. Figure 7a shows a snapshot of the simulated ice-covered profile of CRISSP1D (on January 30, 2002). Figure 7b compares the measured and simulated (Mike-11 and CRISPP1D including and excluding the effect of ice cover) time series of water depth near the upstream boundary (at WSC station 07DA001, near JOSMP site M3). As the figure shows, considering the ice cover effects in the simulations leads to an increase

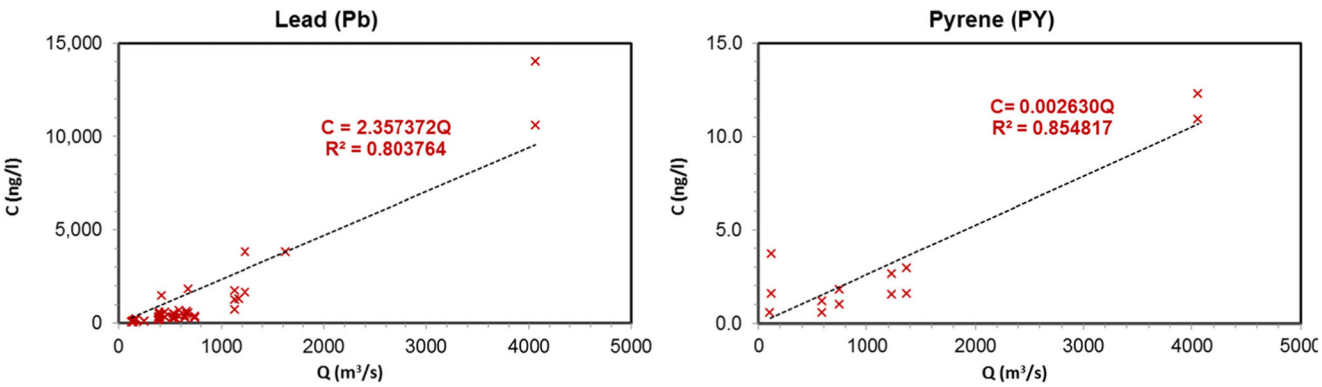

Fig. 5 Examples of rating curves for two of the chemical constituents (one metal and one PAH) at the upstream boundary below Fort McMurray

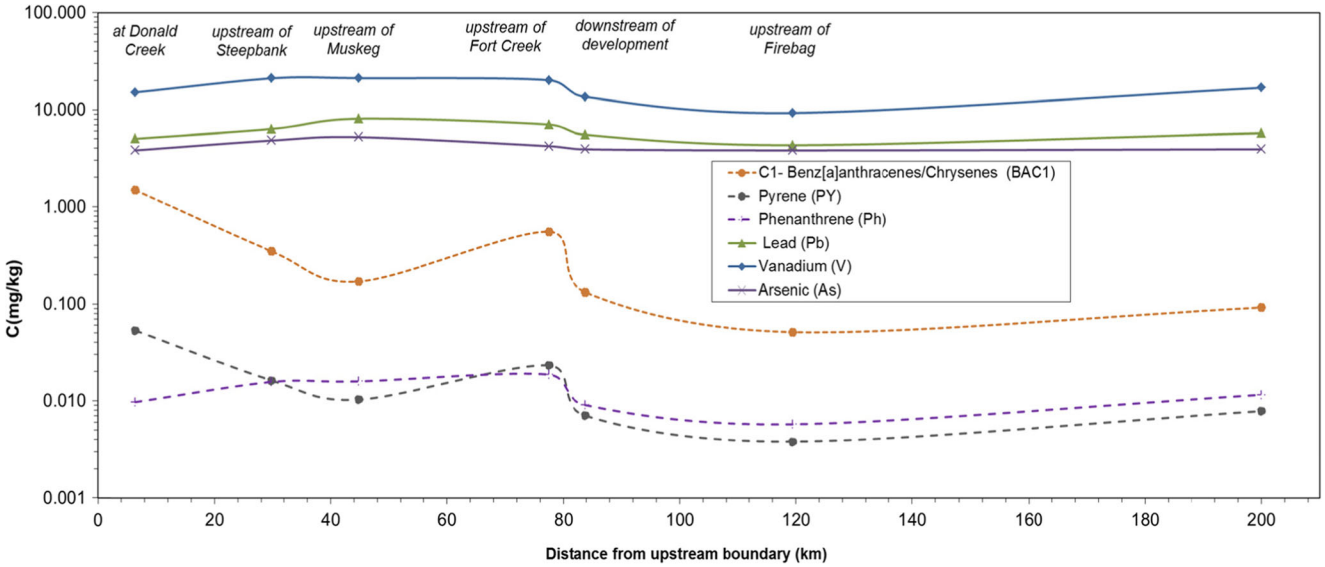

Fig. 6 Longitudinal variation of average measured bed concentration for the different chemical constituents (three metals and three PAHs)

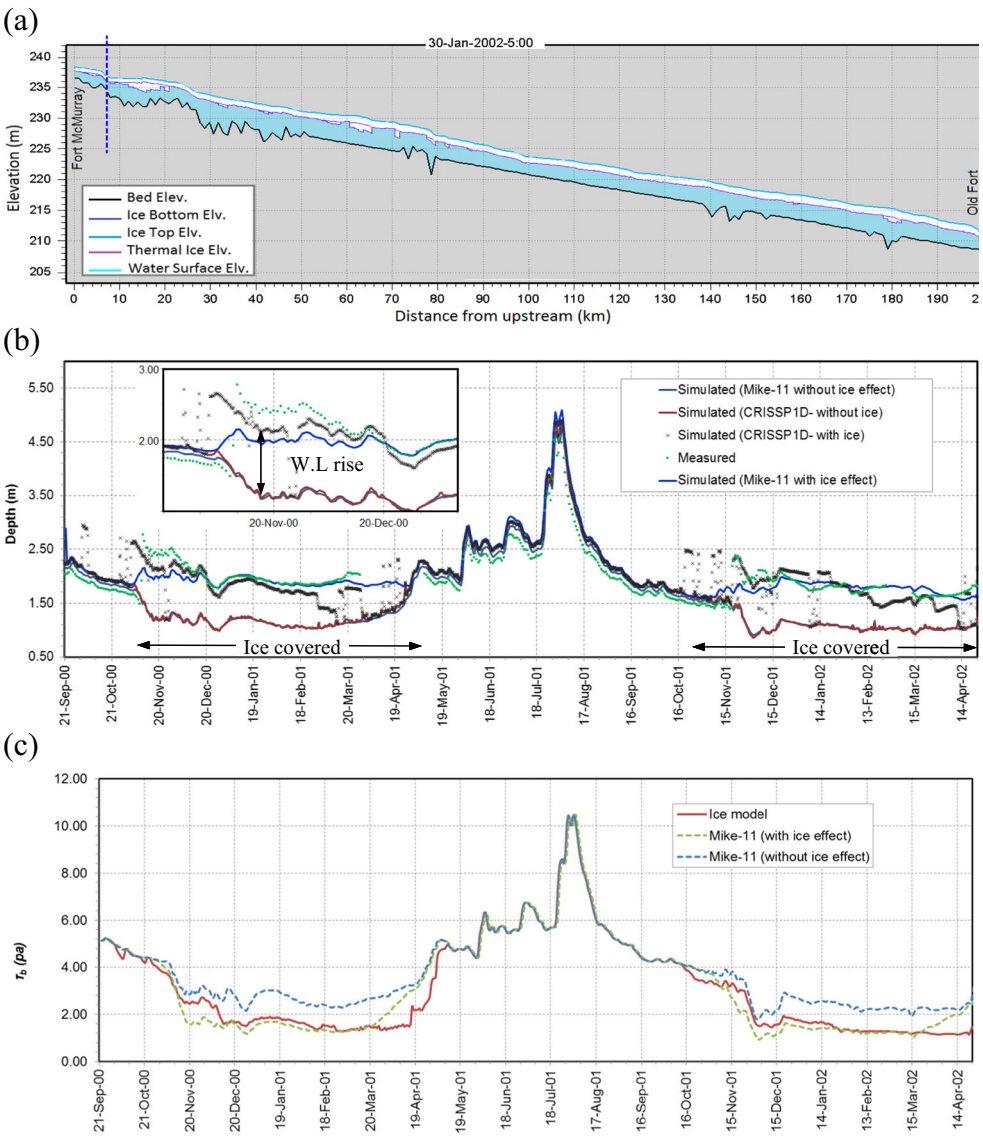

Fig. 7 **a** Snapshot of ice model (CRISSP-1D) longitudinal profiles for Jan. 30, 2002. **b** Time series of measured and simulated water depth near the upstream boundary (at WSC station 07DA001) from the ice model (CRISSP-1D) including/excluding ice simulation, Mike-11 (with and without modifications to account for ice effects). **c** Simulated bed shear stress near the upstream boundary resulted from the CRISSP-1D ice model and Mike-11 (with and without the ice effect)

in the water level during the ice-covered period by about 1 m. The ice coverage generally forms around late October to early November and peaks around mid-April before it eventually melts resulting into open-water condition. The CRISSP1D results show good agreements with the measurements in terms of both the water level and the freeze-up/breakup dates. However, a key factor in the transport of sediment material is the bed shear stress. Since internally coupling the ice model with the Mike-11 sediment transport model was not possible, instead, the Mike-11 model parameters were modified to reproduce the effect of winter ice coverage in terms of both water level and bed shear stress (see Sect. 2.4). Figure 7c compares the time series of the bed shear stress (near the upstream boundary) obtained from the ice model as well as Mike-11 with and without ice effect. The figure shows that, by considering the effect of ice cover, it was possible to reproduce the significant drop in the winter bed shear stress, predicted by the river ice model (CRISPP1D).

5.2 Fine-sediment transport modelling

The time series of the simulated and measured suspended sediment concentration for the LAR at different locations along the study reach are compared in Fig. 8. Note that the concentration values are plotted in a logarithmic scale for a better visual comparison of the order of magnitude in seasonal variations. As the figure shows, the simulated and measured sediment concentrations are generally in a good agreement (with Nash–Sutcliffe efficiency (NSE), value of 0.67 downstream of oil sands developments). Comparison of the simulated and measured sediment-discharge rating curved also

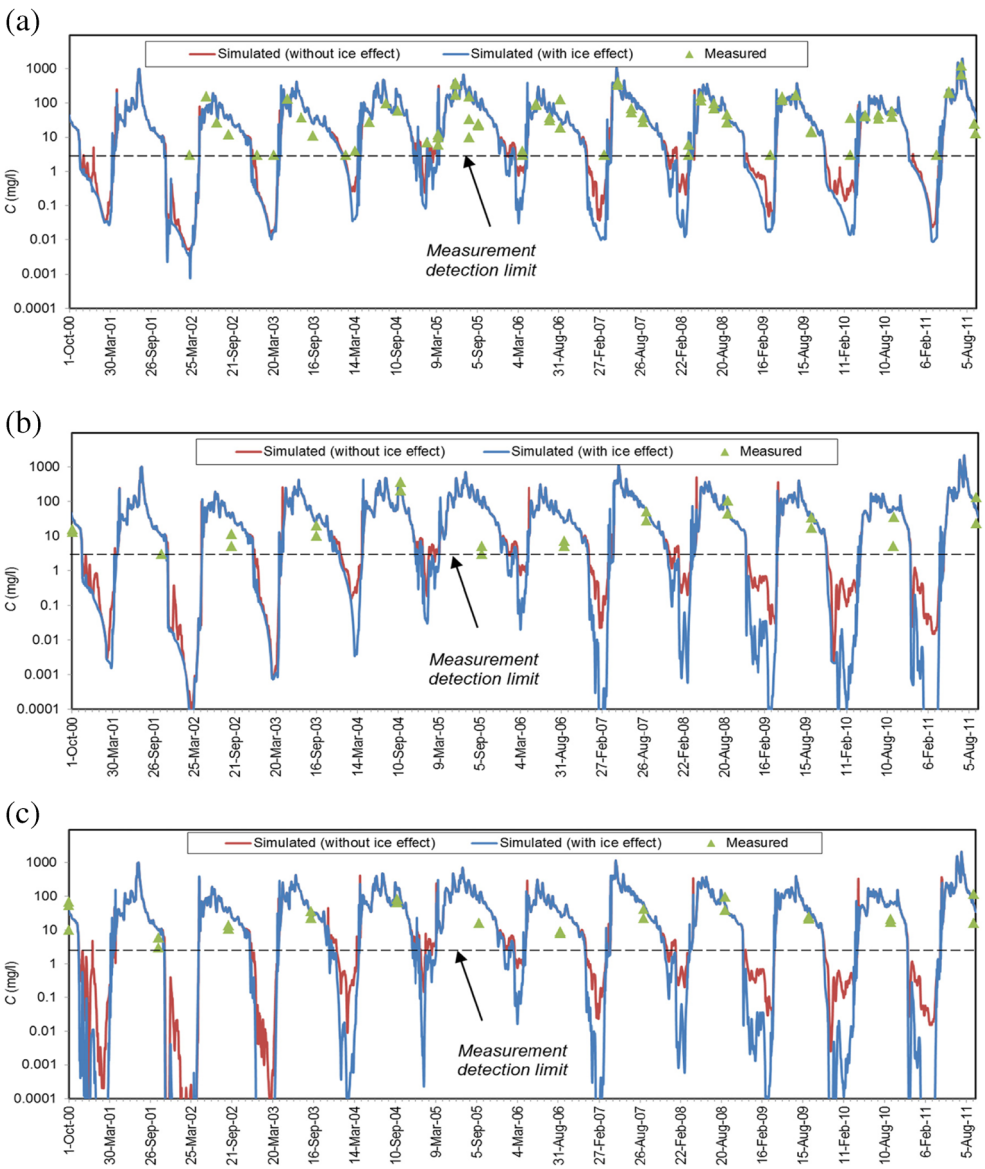

Fig. 8 Time series of measured and simulated (with and without ice effect) suspended sediment concentrations for Athabasca River at **a** downstream of oil sands developments (~85 km from upstream boundary), **b** upstream Muskeg River (~45 km from upstream boundary) and **c** downstream Steepbank River (~30 km from upstream boundary)

shows a good agreement (see Fig. S3 in Electronic Supplementary Material). The maximum suspended sediment concentrations occur during the warmer months of June and July, where the flow rates are also high. The effect of ice cover resulted in a lower sediment concentration value during winter, although the effect is quite small as the bed shear stress corresponding to the winter low-flow condition is relatively low regardless of the presence or absence of ice cover. Comparing Fig. 8a–c, all the three locations show a similar trend in the time series, although slightly lower concentrations are simulated further downstream, especially in low-flow season. Note that the simulation results reflect only the effect of the ice coverage on flow resistance and water depth and have not considered ice dynamic processes during its formation,

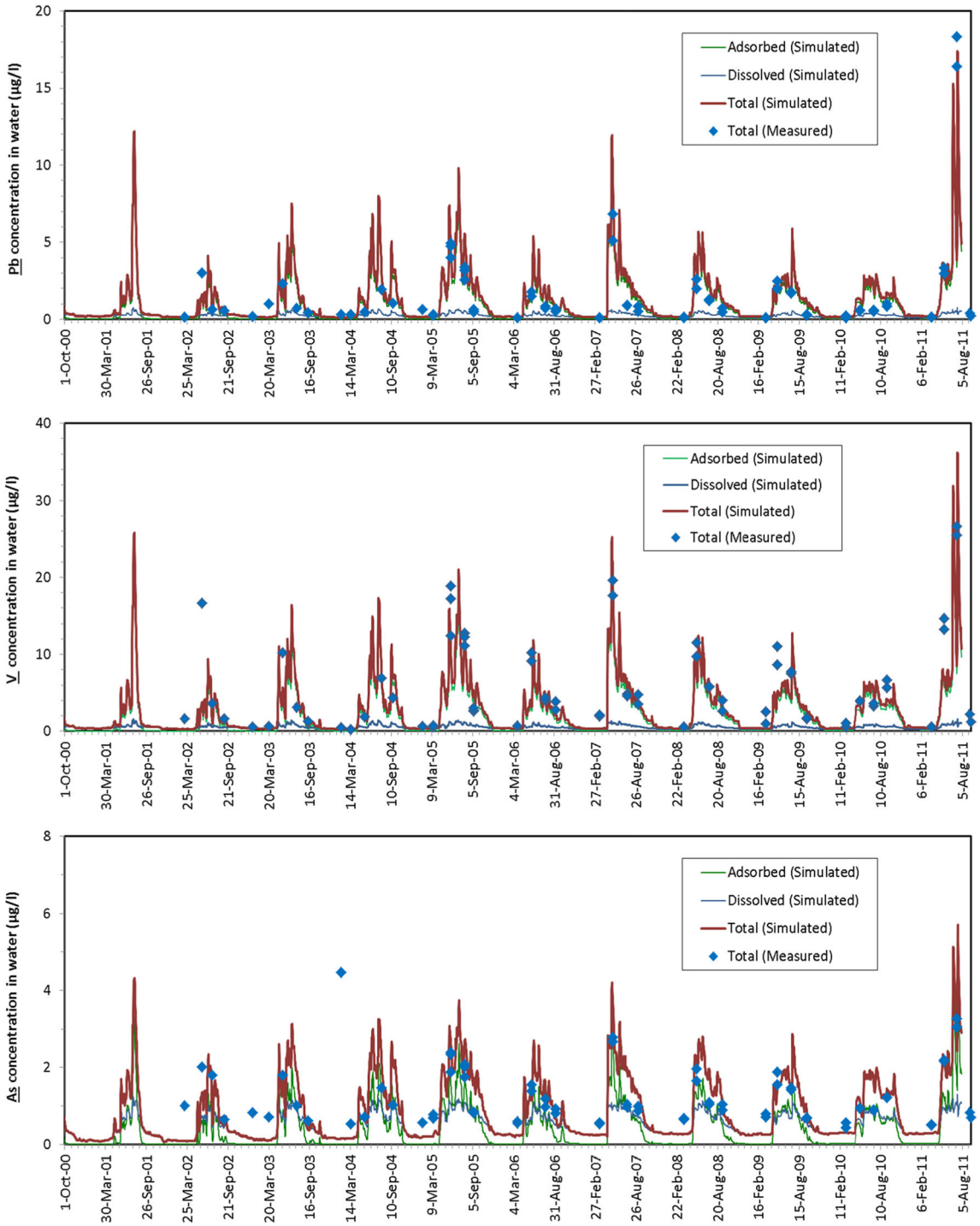

Fig. 9 Time series of dissolved, adsorbed and total metal concentrations in water column at downstream of oil sands development (~85 km from upstream boundary) for lead (Pb), arsenic (As) and vanadium (V)

breakup and some other ice processes that may have additional significant effect on sediment transport.

5.3 Contaminant transport modelling

5.3.1 Temporal variations

Figure 9 shows the time series of simulated dissolved, adsorbed and total (sum of adsorbed and dissolved) concentrations of the three metal constituents, lead (Pb), arsenic (As) and vanadium (V), in water column at a location 85 km from the upstream boundary, which is downstream of the current oil sands development. Measured data for the total concentration of each metal in the water column are also plotted on the same figure. The results show good agreement between total simulated and measured concentrations and that the large proportion of the metals are transported mostly adsorbed to the sediments consistent with the high partitioning coefficient values for these metal constituents. The timings of maximum and minimum metal concentrations in the water column are also

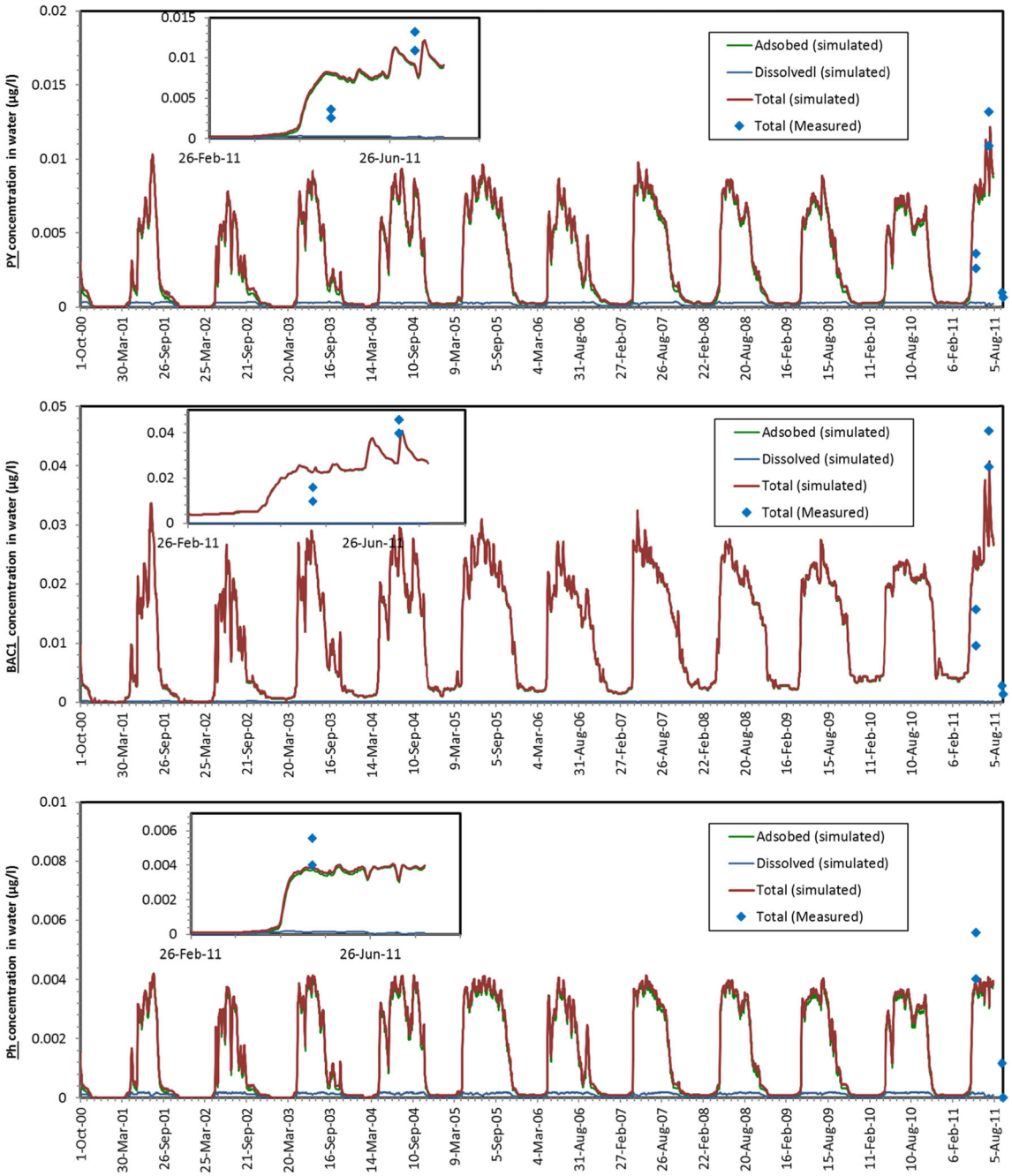

Fig. 10 Time series of dissolved, adsorbed and total PAH concentrations in water column at downstream of oil sands development (~85 km from upstream boundary) for pyrene (PY), phenantrene (Ph) and C1-benz[a]anthracenes/chrysenes (BAC1)

found to be during the high-flow and low-flow seasons, respectively.

Similarly, Fig. 10 shows the time series of simulated dissolved, adsorbed and total concentrations of the three PAHs, pyrene (PY), phenantrene (Ph) and C1-benz[a]anthracenes/chrysenes (BAC1), in water column at the same location downstream of the oil sands development. The very limited measured values of total PAH concentrations in water column (which is available only for the period after 2011) are also plotted on the same figure. The results once again show good agreement between total simulated and measured concentrations. Similar to the case of the metals, the PAH concentration in the water column is mostly found in a form adsorbed to the sediments. To further validate the results, the simulated and measured exceedance probabilities of the total concentration in water column (for the three metals and the three PAHs) are compared in Fig. 11. The exceedance probabilities in simulated and measured concentrations have a good agreement, and

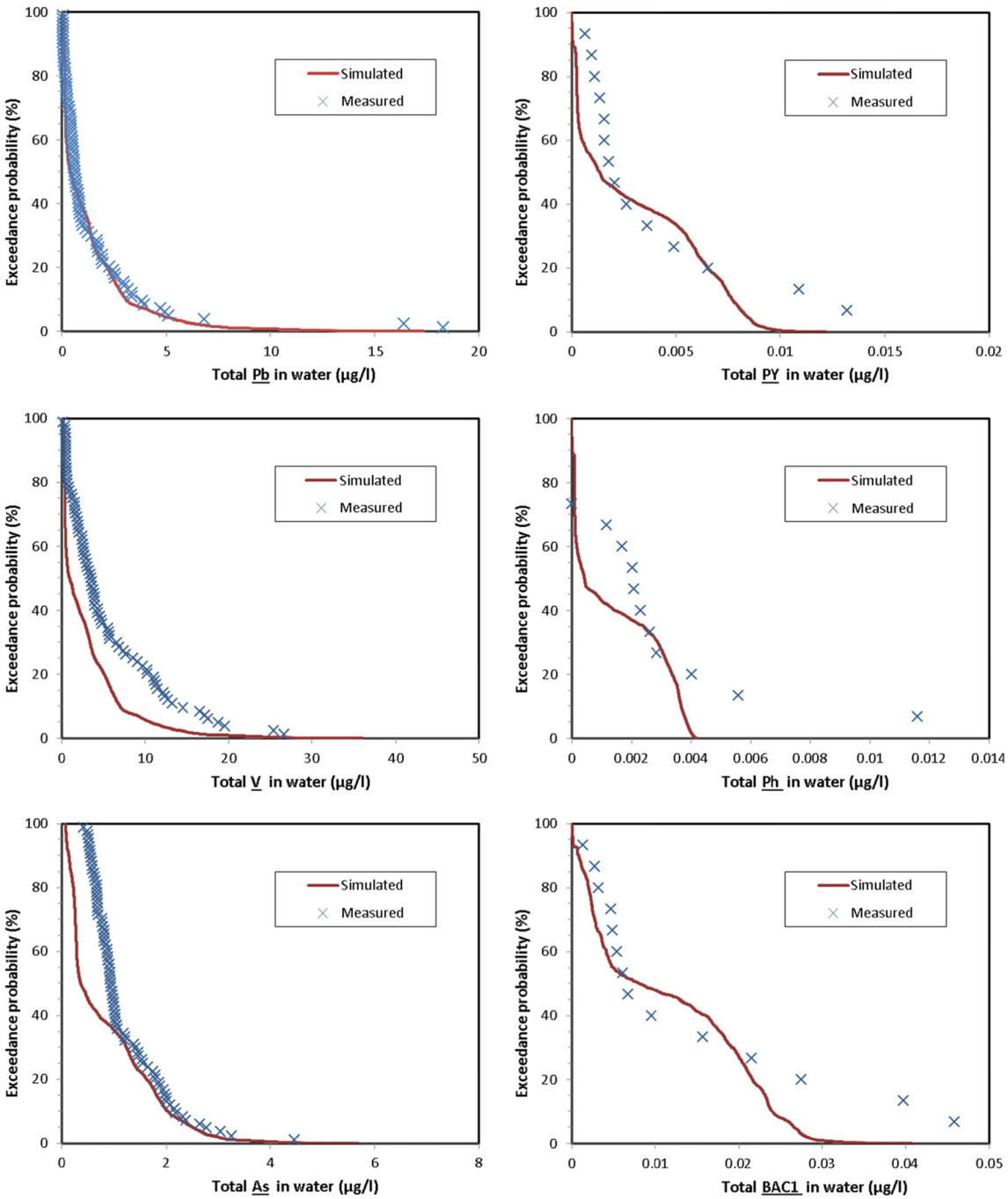

Fig. 11 Exceedance probability of and total concentrations of example metals and PAHs in water column at downstream of oil sands development (~85 km from upstream boundary)

the small discrepancies can be due to the fact that majority of field measurements are conducted in the warm season (corresponding to relatively higher concentrations).

5.3.2 Spatial patterns

To gain some insight into the possible effect of local bitumen deposits and oil sands development on the concentration of chemical constituents in water, the longitudinal (stream-wise) variations in water column concentrations for the selected metals and PAHs are provided in Figs. 12 and 13, respectively. In addition to the average and median annual concentrations, the seasonal averages of three high-flow (open-water) and three low-flow (ice-covered) months are also provided to see the effect of seasonality on the results. Furthermore, the box plots (representing maximum, third quartile, median, first quartile and minimum values) of some limited number of available RAMP and JOSMP measurements are included (note that for PAHs, there are not enough JOSMP measurements to include in the box plots). Despite the fact that the available measurements are very scattered and not evenly distributed throughout the year, they can provide an insight into the overall patterns and the range of concentrations of the various chemical constituents in the region.

As the figures show, the simulated and measured concentrations have similar spatial patterns and ranges. The spatial

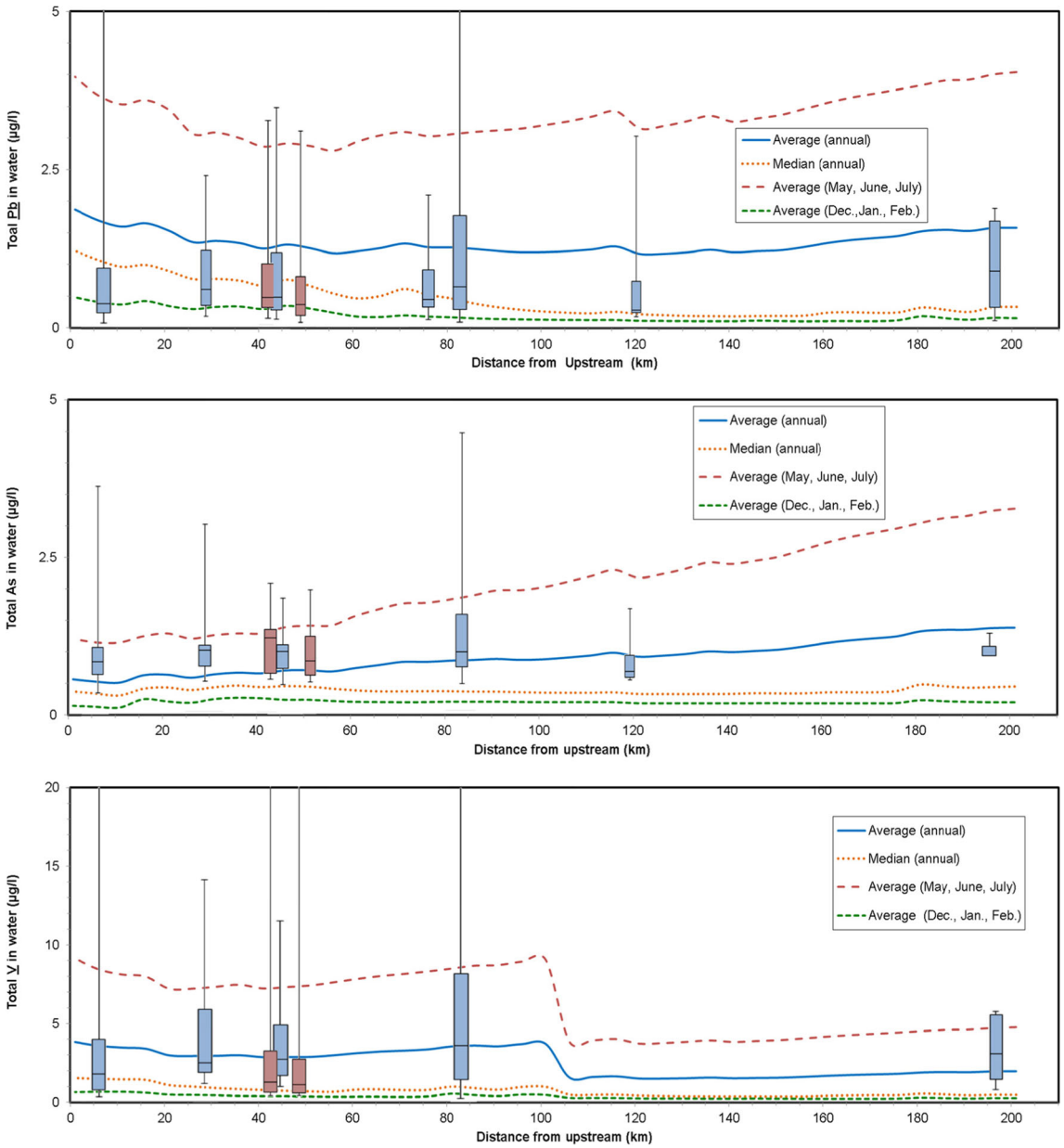

Fig. 12 Longitudinal variation of concentration of metals including lead (Pb), arsenic (As) and vanadium (V) in water column. *Box plots* (min, first quartile, median, third quartile and max) correspond to the available measured data (*blue*: RAMP data, *brown*: JOSMP data)

patterns of the annual average concentration values suggest an overall increase from upstream (Ft. McMurray) to downstream (Old Fort) reaches of the river. There is also a strong seasonality in the magnitude and direction of the longitudinal patterns. While the high-flow open-water season results show the relatively high average values and an overall increase in concentration from upstream to downstream, the cold ice-covered season shows relatively low average concentration values with some longitudinal variations, especially for metals (e.g. Pb, V and As). The average concentration in As and Pb shows a slight increase from upstream to downstream direction, while the concentration of V increases for the first ~100 km (up to downstream of the oil sands developments) and then it decreases. The concentrations of PY, Ph and BAC1 have a pattern similar to V (with an increase up to downstream of the oil sands developments and then a slight decrease). The average concentration of Ph shows less variation than PY and BAC1. In general, the high-flow season appears to be the most important period for the transport of these chemical constituents. Comparing Figs. 12 and 13 with Fig. 6, one can also see that the longitudinal variations of simulated concentration in water column are strongly related to the pattern of the corresponding bed concentration (i.e. an important source of chemicals).

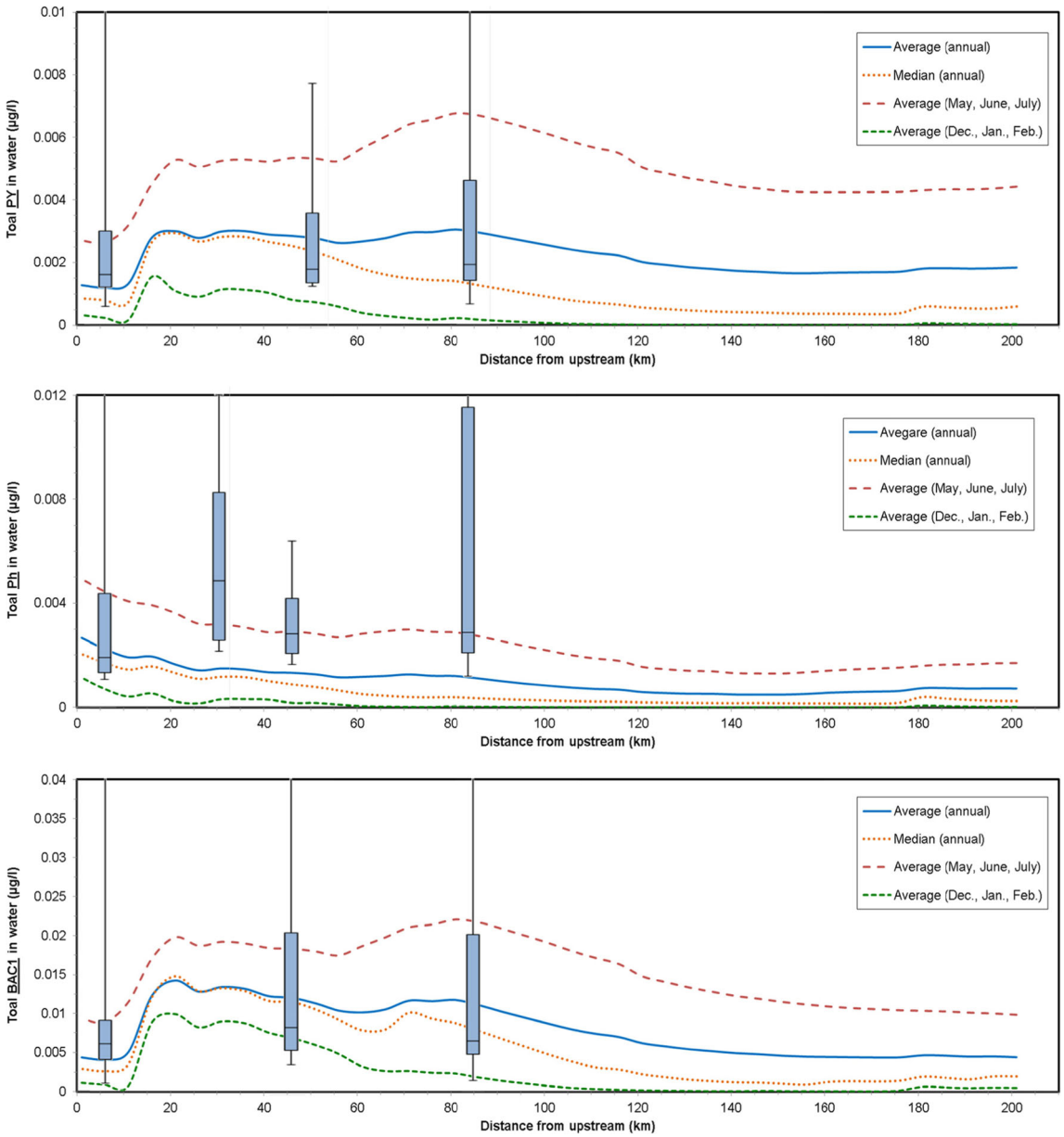

Fig. 13 Longitudinal variation of concentration of PAHs including in water column. *Box plots* (min, first quartile, median, third quartile and max) correspond to the available measured data (RAMP data)

5.4 Scenario-based simulation

The hydrodynamic and transport models of the LAR are applied to investigate the effect of various hypothetical pollution scenarios on the transport regime within the river system. Table 3 summarizes the different high concentration chemical constituent inflow scenarios considered in this study. The first set of scenarios considers increases (10 and 100 times observed values) in the concentration of chemicals entering the LAR from the Muskeg and Ells Rivers. The second set of scenarios considers 2 days (48 h) of chemical spill (approximately equivalent to 5 million l of raw bitumen) into the Muskeg River during mean flow condition of July 20, 2001 (such spill is assumed to contain 170 μg l^{-1} lead and 25 μg l^{-1} PY to Muskeg). The selection of these two tributaries is based on their proximity to the developments and past incidences (e.g. those reported by Timoney and Lee 2009). The hydrodynamic and transport model is run with each of these hypothetical tributary chemical inflow scenarios while keeping all other model parameters and boundary conditions the same as in the reference simulation.

Table 3 shows the effect of each pollution scenario on the simulated concentration of chemicals at the outflow (downstream) boundary near Old Fort compared to the corresponding values for the reference condition. Figure 14 also shows the effect of the first four tributary inflow scenarios on the longitudinal variations of water column chemical concentrations along the LAR. The scenario with 10 times increase in the concentration of lead (Pb) and pyrene (PY) in the Ells River resulted in increases in the LAR water column concentration of the same chemicals by 5.5 and 17.4% at 10 km downstream of the confluence and less than 5% at the downstream outflow boundary near Old Fort, respectively, while the 100 times increase resulted in the corresponding increases of 48.4 and 135.2% at 10 km downstream of the confluence and 17 and 35.5% at the downstream outflow boundary, respectively. Similar but slightly less increases are also simulated in the LAR for the increases in Pb and Py in the Muskeg River. The main messages from these scenario simulation results are (1) While a large and sustained increase (e.g. 100 times the reference values) in the concentration of chemicals in tributary streams will have a noticeable impact on the water column concentrations throughout the Athabasca mainstem downstream of each confluence, the effect of a relatively smaller increase (e.g. up to 10 times the reference values) in tributary inflow concentration may not be high and would be limited to locations immediately downstream of the confluence. (2) The impact of any increase in the inflow concentration of tributaries diminishes further downstream of each confluence due to depositional and other processes in the river mainstem. (3) The effect of increased inflow concentration will also be higher in case of tributaries with higher discharge compared to those with lower discharge (Ells compared to Muskeg in this study). Note that the tributary contributions of chemicals may not mix fully in the mainstem due to the near-bank depositions that are not seen by the 1D models that provide cross-sectional averaged values.

Figure 15 shows the time series of water column concentrations of pyrene (PY) and lead (Pb) at various distances along the LAR mainstem downstream of the spill location corresponding to the hypothetical "Muskeg-Spill" scenario. The results show the significant impact of such spills on the concentration of chemicals in the main river channel, with increases well over 300% immediately downstream of the confluence. The effect, however, diminishes further downstream of the spill location, as part of the chemical constituents settles to the bottom of the channel, while the rest is diluted within the river. The results show a 4-day time lag

Table 3 Summary of hypothetical contamination scenarios and their effects on the LAR (for two locations) compared to the reference condition

Scenarios		10 km downstream of tributary confluence						Downstream (outflow) boundary					
		Reference value (μg l^{-1})		Scenario value[a] (μg l^{-1})		Increase (%)		Reference value (μg l^{-1})		Scenario value[a] (μg l^{-1})		Increase (%)	
Name	Description	Pb	PY	Pb	PY	Pb	PY	Pb	PY	Pb	PY	Pb	PY
Ells-10×	10 times increase in Ells River conc.	1.28	1.280.00298	1.35	0.00350	5.5	17.4	1.58	0.001843	1.62	0.00194	2.5	5
Ells-100×	100 times increase in Ells River conc.			1.9	0.00701	48.4	135.2			1.85	0.0025	17	35.5
Muskeg-10×	10 times increase in Muskeg River conc.	1.18	0.00263	1.31	0.00280	11.0	6.5			1.6	0.00188	1.3	2.5
Muskeg-100×	100 times increase in Muskeg River conc.			1.46	0.00349	23.7	32.7			1.67	0.00194	5.7	5.5
Muskeg-Spill	A 2-day spill in Muskeg River in mean flow condition.	1.56	0.00363	6.83	0.01782	338.1	390.9	1.20	0.003687	2.02	0.00805	40.5	54.2

[a] For "Muskeg-Spill" scenario, the provided values are spill peak value, while for other scenarios, they are values averaged over the 11-year simulation period

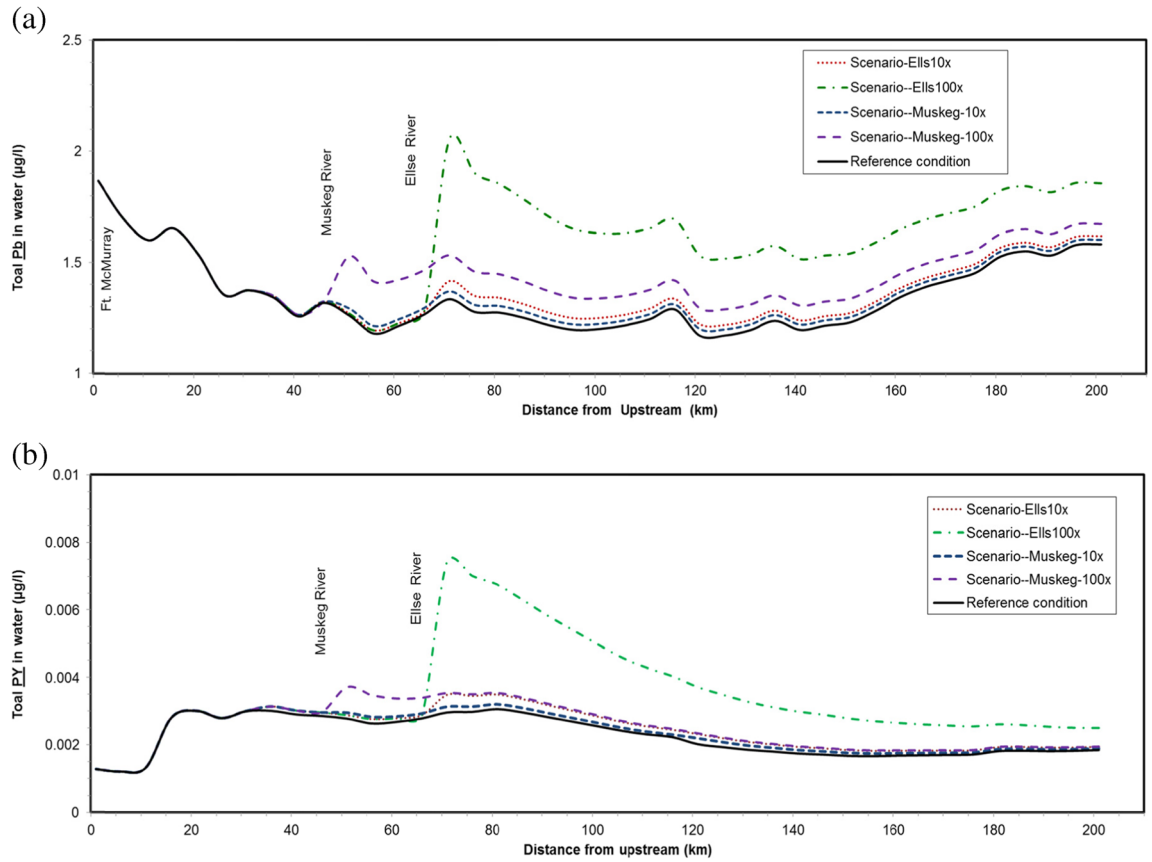

Fig. 14 Effect of various tributary inflow scenarios on the mean longitudinal variations of **a** lead (Pb) and **b** pyrene (PY) concentrations

for the Pb spill peak to reach the downstream boundary. However, since its natural concentration value can sometime be relatively higher, the effect of this particular Muskeg-Spill scenario may not be out of the ordinary. The corresponding time lag for PY is 2 weeks, and the effect of the Muskeg-Spill scenario is much more significant compared to the natural condition. The difference in the time lag of Pb and PY can be due to the difference in their properties (e.g. their partitioning coefficients) or their initial content in the river water column and bed. It should be noted that the 1D model shows the cross-sectional average values and does not account for the lateral variations and cannot capture the deposition of sediments and associated chemicals in low-flow regions such as pools and shallow floodplains; therefore, the chemicals from an actual spill may stay much longer within the study reach.

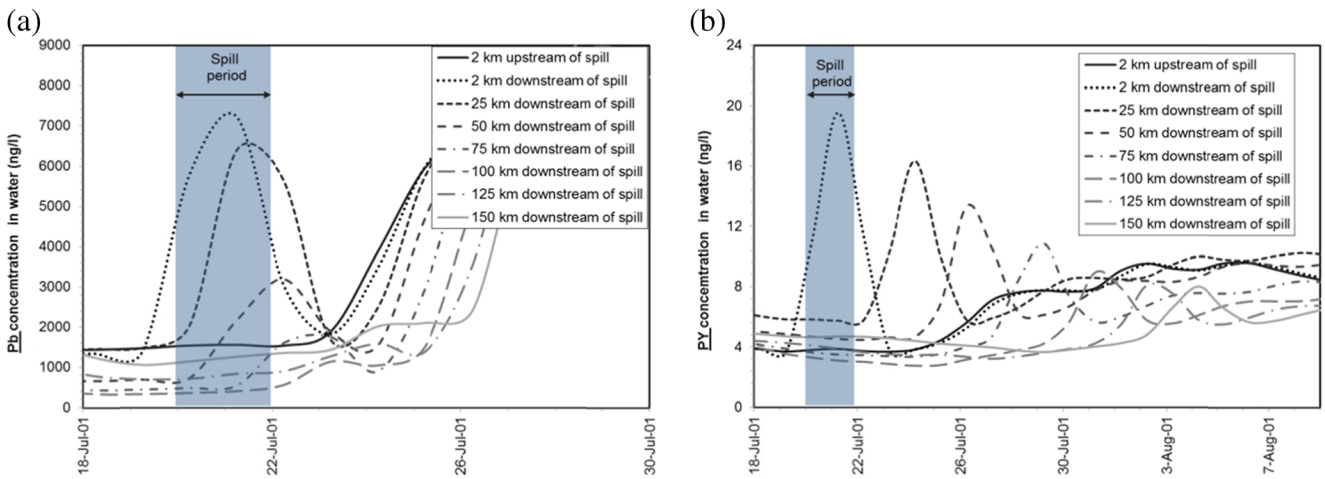

Fig. 15 Effect of various the "Muskeg-Spill" hypothetical scenarios on the time series of **a** lead (Pb) and **b** pyrene (PY) concentrations, for various distances from spill locations

6 Conclusions

An integrated deterministic numerical modelling framework for simulation of the spatial and temporal variation in the sediment and associated chemical constituents within the LAR was developed. The framework was based on the Mike-11 hydrodynamics, CST and contaminant transport models. These models were externally coupled with the 1D ice process models, CRISSP-1D, to account for the cold season effects. The models were calibrated and validated for ~200-km reach of the Lower Athabasca River (LAR) for the period of 2000–2011 using the available measurements. The models were subsequently applied to assess the effects of various hypothetical pollution scenarios on the concentration of constituent chemicals in the river system.

The simulation results successfully reproduced the hydrodynamics and sediment transport patterns as well as the state and variation of selected metal and PAH constituents (i.e. As, Pb, V, PY, Ph, BAC1). The results indicated a slight overall decline in suspended sediment concentrations during the winter ice cover season. They also showed that the high-flow season is a key period for transport of chemical constituents in the river. The other important finding is that the initial concentration of each chemical constituent in the bed sediment determines the overall state and variation of each chemical constituent in the water column. The results of the hypothetical pollution scenarios showed that the increases in the concentrations of chemical constituents in tributary streams (e.g. in Ells River and Muskeg River) have to be very high to have a significant effect on their corresponding water column concentration in the LAR. The effects are also found to be high only within the immediate vicinity of the tributary confluences and gradually diminish with distance to the downstream outflow boundary. The short-time spill scenario in the Muskeg River was also found to have a significant effect on downstream water column concentrations in LAR especially for PY.

The numerical modelling framework developed in this study and some of the results presented can be extended for modelling of other chemical constituents. It can be used as a valuable tool and guideline for future environmental assessment and monitoring of the LAR ecosystem such as to determine the locations and time of the future water quality samplings. Suggestion for future researches is to apply the developed framework for additional scenario (such as future climate and loading scenarios)-based studies to investigate possible future states of sediment and contaminant transport in the river. Also, considering the inability of 1D models in prediction of lateral variations (such as near bank depositional patterns), the application of a 2D model is recommended for a more detailed analysis of sediment and constituent chemical transport within the LAR.

Acknowledgements The financial support for this study was provided by the Government of Alberta and Environment Canada Joint Oil-Sands Monitoring Program (JOSMP). The authors would like to thank Drs. Fred Wrona, Anil Gupta, Spyros Beltaos, Patricia Chambers and Malcolm Conly for their comments and support at the different stages of this project. The authors acknowledge Dr. Hyung-Il Eum for his help in providing the Athabasca River hydrological modelling data, Tom Carter and Jennifer Pesklevits for collecting and processing the GeoSwath data, Dr. Fay Hicks for providing some of the Lower Athabasca River cross-sectional data and Martin Jasek for his comments and helps with the CRISSP1D model. The authors would also like to thank Dr. Roderick Hazewinkel from Alberta Environment and Parks for facilitating access to the LiDAR data used in preparing the bathymetry for the Athabasca River and its flood plains.

References

Akre CJ, Headley JV, Conly FM, Peru KM, Dickson LC (2004) Spatial patterns of natural polycyclic aromatic hydrocarbons in sediment in the lower Athabasca River. J Environ Sci Heal A 39(5):1163–1176

Andrishak R, Abarca JN, Wojtowicz A, Hicks F (2008) Freeze-up study on the Lower Athabasca River (Alberta, Canada). Proc. 19th IAHR Ice Symposium. Vancouver, Canada 1:77–88

Canada-Alberta Joint Oil-Sands Monitoring Program (2012)

Canada-Alberta Joint Oil Sands Monitoring Portal (JOSMP) (2015) http://www.jointoilsandsmonitoring.ca. Accessed 10 Oct 2015

Canadian Council of Ministers of the Environment (CEMA) (2012) Lower Athabasca data. http://ftp.cciw.ca/incoming/LowerAthabasca_data_March05.12/. Accessed 10 Nov 2012

Conly FM, Crosley RW, Headley JV (2002) Characterizing sediment sources and natural hydrocarbon inputs in the lower Athabasca River, Canada. J Environ Eng Sci 1(3):187–199

Conly FM, Crosley RW, Headley JV, Quagraine EK (2007) Assessment of metals in bed and suspended sediments in tributaries of the Lower Athabasca River. J Environ Sci Health 42(8):1021–1028

Danish Hydraulics Institute (DHI) (2012) MIKE11 user guide & reference manual. Danish Hydraulics Institute, Horsholm

Droppo IG, Krishnappan BG (2014) Cohesive sediment transport—part I: a modelling approach. Under Environment Canada Internal Review

Droppo IG, D'Andrea L, Krishnappan BG, Jaskot C, Trapp B, Basuvaraj M, Liss SN (2014) Fine-sediment dynamics: towards an improved understanding of sediment erosion and transport. J Soils Sediments 15(2):467–479

Environment Canada (EC) Climate Database (2013) http://climate.weather.gc.ca. Accessed 10 Sept 2013

Ettema R, Daly SF (2004) Sediment transport under ice. ERDC/CRREL TR-04-20. Cold Regions Research and Engineering Laboratory, US Army Corps of Engineers

Eum HI, Dibike YB, Prowse TD (2014) Uncertainty in modelling the hydrologic responses of a large watershed: a case study of the Athabasca River Basin, Canada. Hydrol Process 28(14):4272–4293

Garcia-Aragon J, Droppo IG, Krishnappan B, Trapp B, Jaskot C (2011) Experimental assessment of Athabasca River cohesive sediment deposition dynamics. Wat Qual Res J Can 46(1):87–96

Geobase (2012) http://www.geobase.ca/geobase/en/index.html. Accessed Oct 2012

Ghosh U, Gillette JS, Luthy RG, Zare RN (2000) Microscale location, characterization, and association of polycyclic aromatic hydrocarbons on harbour sediment particles. Environ Sci Technol 34:1729–1736

Hall RI, Wolfe BB, Wiklund JA, Edwards TW, Farwell AJ, Dixon DG (2012) Has Alberta Oil-Sands development altered delivery of polycyclic aromatic compounds to the Peace-Athabasca Delta? PLoS One 7(9):e46089

Headley JV, Akre C, Conly FM, Peru KM, Dickson LC (2001) Preliminary characterization and source assessment of PAHs in tributary sediments of the Athabasca River, Canada. Environ Forensic 2(4):335–345

Hicks F (2011) Personal Communication (2011)

Kashyap S, Oveisy A, Shakibaeinia A, Dibike YB, Prowse TD, Droppo IG (2014) Numerical modeling of flow and sediment transport within the lower reaches of the Athabasca River: a case study. Proc. HIC 2014, 11th International Conference on Hydroinformatics, New York, USA

Kelly EN, Schindler DW, Hodson PV, Short JW, Radmanovich R, Nielsen CC (2010) Oil-sands development contributes elements toxic at low concentrations to the Athabasca River and its tributaries. Proc Natl Acad Sci 107(37):16178–16183

Khanna VK, Herrera WV (2003) Comparison of the one-D and cdg1-D models in the lower Athabasca River basin to estimate high flows during open-water season. Environment Canada Report

Knack I, Shen HT (2015) Sediment transport in ice-covered channels. Int J Sediment Res 30(1):63–67

Pietroniro A, Hicks F, Andrishak A, Watson D, Boudreau P, Kouwen N (2011) Hydraulic routing of flows for the Mackenzie River, Environment Canada, University of Alberta & National Research Council of Canada

Prowse TD (2001) River-ice ecology. I: hydrologic, geomorphic, and water-quality aspects. J Cold Reg Eng 15(1):1–16

Regional Aquatics Monitoring Program (RAMP) (2013) Monitoring database: sediment quality. http://www.ramp-alberta.org/data/Sediment/sediment.aspx (Nov. 2013)

Shakibaeinia A, Kashyap S, Dibike YB, Prowse TD (2016) An integrated numerical framework for water quality modelling in cold-region rivers: a case of the lower Athabasca River. Sci Total Environ 569:634–646

Shen HT (2005) CRISSP1D programmer's manual. Prepared by Department of Civil Engineering, Clarkson University, Potsdam, NY for CEA Technologies Inc. (CEATI). CEATI Report No. T012700-0401

Timoney KP, Lee P (2009) Does the Alberta tar sands industry pollute? The scientific evidence. Open Conserv Biol J 3:65–81

Van Rijn LC (1984) Sediment transport, part I: bed load transport. J Hydraul Eng 110(10):1431–1456

Water Survey of Canada (WSC) (2013) Hydat database. https://www.ec.gc.ca/rhc-wsc/default.asp?lang=En&n=9018B5EC-1. (July, 2013)

Wiklund JA, Hall RI, Wolfe BB, Edwards TW, Farwell AJ, Dixon DG (2014) Use of pre-industrial floodplain lake sediments to establish baseline river metal concentrations downstream of Alberta Oil-Sands: a new approach for detecting pollution of rivers. Environ Res Lett 9(12):124019

Wrona FJ, Carey J, Brownlee B, McCauley E (2000) Contaminant sources, distribution and fate in the Athabasca, Peace and Slave River Basins, Canada. J Aquat Ecosyst Stress Recover 8(1):39–51